Nonisothermal Curing of a Solid Resole Phenolic Resin

Da-Peng Zhou,[1] Siping Du,[2] Liqiong Yu,[3] Zheng Liu[3]

[1]*Biochemistry and Chemical Engineering Department, Jiaxing College, Jiaxing 314001, People's Republic of China*
[2]*Jiaxin Chenghe New Materials Company, Limited, Jiaxing 314027, People's Republic of China*
[3]*Zhejiang Jiamin Plastics Company, Limited, Jiaxing 314027, People's Republic of China*

Received 16 July 2010; accepted 5 November 2010
DOI 10.1002/app.33775
Published online 11 March 2011 in Wiley Online Library (wileyonlinelibrary.com).

ABSTRACT: A commercial solid resole phenolic resin was thoroughly characterized with Fourier transform infrared spectroscopy, NMR, and gel permeation chromatography, and its nonisothermal curing reaction was studied systematically with differential scanning calorimetry at a series of heating rates (βs) of 3, 4.5, 5.7, and 10°C/min. The results show that the solid resole had a higher molecular weight than conventional liquid resoles, and its reactive hydroxymethyl (CH_2—OH) and dibenzyl ether (CH_2—O—CH_2) functionalities participated in the crosslinking reaction upon heating. The nonisothermal curing reaction of the solid resole exhibited a relatively constant reaction heat, whereas the onset, peak, and end curing temperatures increased gradually with increasing βs. In addition, the reaction kinetics of the solid resole was analyzed with an *n*th-order reaction model, the global activation energy was determined with the Kissinger method, and the reaction order was derived from the Crane equation. The obtained rate equation was applied to simulate the reaction time, conversion, and reaction rate, with a good fit achieved between the experimental data and the model predications. In conclusion, this study provided us with new knowledge on solid resoles at a molecular level and was also a great help for the curing procedure design, property optimization, and practical application of this commercial solid resole. © 2011 Wiley Periodicals, Inc. J Appl Polym Sci 121: 1938–1945, 2011

Key words: activation energy; curing of polymers; differential scanning calorimetry (DSC)

INTRODUCTION

Phenolic resins are widely used thermosetting polymers because of their excellent flame retardance, temperature resistance, mechanical strength, electrical insulation, dimensional stability, and relatively low manufacturing cost.[1–6] Their primary applications are in construction materials, electronics, aerospace, molded parts, insulating varnishes, laminated sheets, industrial coatings, fiber bonding, wood products, and automotive industries.[7–9] Phenolic resins generally fall into two main classes, resole and novolac, in terms of their molecular structures and synthesis conditions.[1,10,11] For example, resole phenolic resins are conventionally prepared by the reaction of excessive formaldehyde with phenol under alkaline conditions to produce a soluble and fusible prepolymer (resole) with many hydroxymethyl (CH_2—OH) functionalities located at the phenol nucleus of the backbone. On the other hand, with an acid catalyst, the polycondensation of phenol and insufficient formaldehyde produces novolac oligomers, which bear essentially no CH_2—OH groups. Resoles can be hardened to form a crosslinked thermosetting polymer by heating alone primarily because of the reactive nature of CH_2—OH groups toward the phenol nucleus, whereas novolacs have to copolymerize with a curing agent, such as hexamethylenetetramine, to achieve crosslinking on heating.[12–14]

Sometimes, resoles are desirable for achieving superior overall properties because there is no release of corrosive violate amine compounds during curing and improved heat resistance, which arises from a higher crosslinking density without the introduction of any amine linkages, such as in a hexamethylenetetramine-cured novolac network. Historically, resoles are usually in liquid form with a very low molecular weight; this is due largely to easy gelation in their manufacturing processes. However, liquid resoles lack storage stability, are hard to handle, and need to be stabilized by solvents; this greatly limits their applications.[15,16] To overcome these drawbacks, it is desirable to use solid resoles to replace liquid ones, especially in high-performance phenolic molding materials. Thanks to recent breakthroughs in the manufacturing techniques of resoles, solid resole products have become available commercially in the international market. To our knowledge, however, basic scientific studies on solid resoles have received little attention until now, although there is abundant literature on liquid resoles.[15,17–24] Furthermore, the curing reactions of a thermosetting polymer have a

Correspondence to: D.-P. Zhou (zdp9270@163.com).
Contract grant sponsor: Jiaxing City Science and Technology Program; contract grant number: 2009AY201.

fundamental influence on their curing cycle design, quality control, processing, property optimization, and application areas. To this end, it is very necessary to gain a comprehensive understanding of the curing reactions of solid resoles from a practical application viewpoint.

In this study, we focused on the characterization and curing reactions of a commercial solid resole phenolic resin. The molecular structure, molecular weight, and molecular weight distribution of the solid resole were characterized systematically by Fourier transform infrared (FTIR) spectroscopy, NMR, and gel permeation chromatography (GPC), and the nonisothermal curing reactions were investigated with a dynamic differential scanning calorimetry (DSC) technique.

EXPERIMENTAL

Materials

The solid resole phenolic resin was obtained from Gun EI Chemical Industry Co., Ltd. (Shukuoruimachi, Japan) and was prepared via an advanced suspension polymerization technique. The resole was a fine yellow powder and was dehydrated *in vacuo* at room temperature for 2 h before the experiments. Other materials were bought from the Chinese domestic market and were used directly without further treatment.

Instrumentation

The FTIR spectra of the solid resole and its cured product were recorded on a Nicolet-560 IR spectrometer (Nicolet, Madison, USA) over the wave-number range 400–4000 cm^{-1}.

^{1}H-NMR and ^{13}C-NMR data of the resole were collected on an AVANCE DMX400 spectrometer (Rheinstetten, Germany) (400 MHz) with hexadeuterated dimethyl sulfoxide (DMSO-d_6) as the solvent and tetramethylsilane as the internal standard.

Heat-flow rates as a function of temperature of the resole were registered on a differential scanning calorimeter (DSC200F3, Netzsch, Selb, Bavaria, Germany) with an intercool under protective nitrogen (60 mL/min) and purge nitrogen (30 mL/min) at four heating rates ($\beta s = 3$, 4.5, 6.7, and 10°C/min) at 50–220°C. The temperature and sensitivity of DSC were previously calibrated with a set of high-purity standard metals (Hg, In, Sn, Bi, and Zn), and the collected thermal data were processed with Netzsch Proteus software. About 5 mg of the solid resole was enclosed in an aluminum DSC capsule and subjected to a dynamic DSC temperature scan with an identical capsule as the reference.

The molecular weight and molecular weight distribution of the solid resole were analyzed with a Waters 1525 (Massachusetts, USA) gel permeation chromatograph equipped with a 2489 UV detector (254 nm), a 2412 reflection detector, and a series of Styragel HR_{1-3} ($\Phi 7.8 \times 300$ mm) columns. The equipment was calibrated with polystyrene standards of known molecular weights with monodistributions, and the collected GPC data was processed with the Waters Breeze software package. An amount of 20 μL of the solid resole in tetrahydrofuran (0.3 wt %) was injected into the GPC to start measurement with tetrahydrofuran as the eluent (1.0 mL/min).

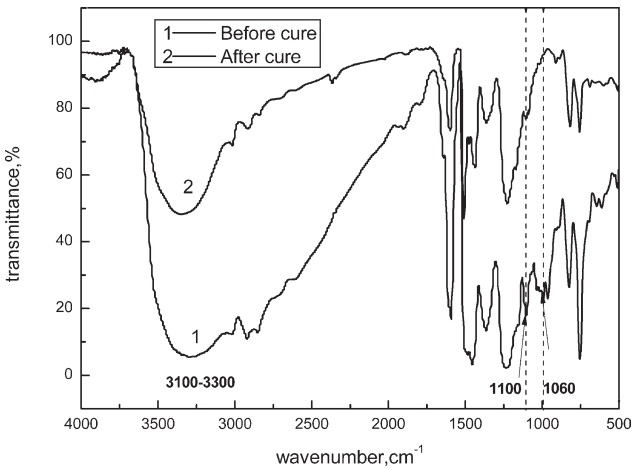

Figure 1 FTIR spectra of the solid resole.

RESULTS AND DISCUSSION

Characterization of the solid resole

FTIR

The general molecular structures of the resole and its cured product were analyzed with FTIR spectroscopy on a KBr pellet. Figure 1 presents the IR spectra of the solid resole and its cured product. The IR absorption peaks of the CH_2—OH units and the characteristic bands of dibenzyl ether (CH_2—O—CH_2) segments were located at about 1100 and 1060 cm^{-1}, respectively. After curing, the absorption band of the CH_2—OH and CH_2—O—CH_2 moieties essentially disappeared, whereas the IR absorption of —OH decreased dramatically. These observations suggest that the solid resole possessed two kinds of reactive species in its molecules: CH_2—OH and CH_2—O—CH_2 functionalities. Upon heat curing, both functionalities could participate the curing reaction to form the diphenylmethylene bridges, which simultaneously gave off water.[25]

NMR

To explore its molecular structures in more depth, NMR was used to derive information about the

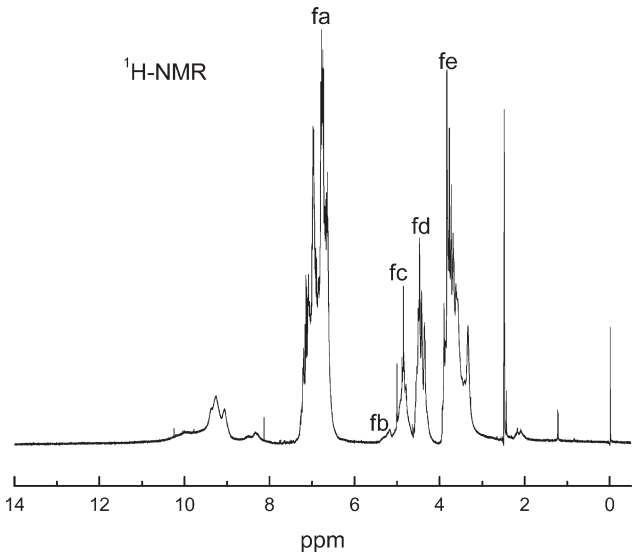

Figure 2 ^{1}H-NMR spectrum of the solid resole (before curing).

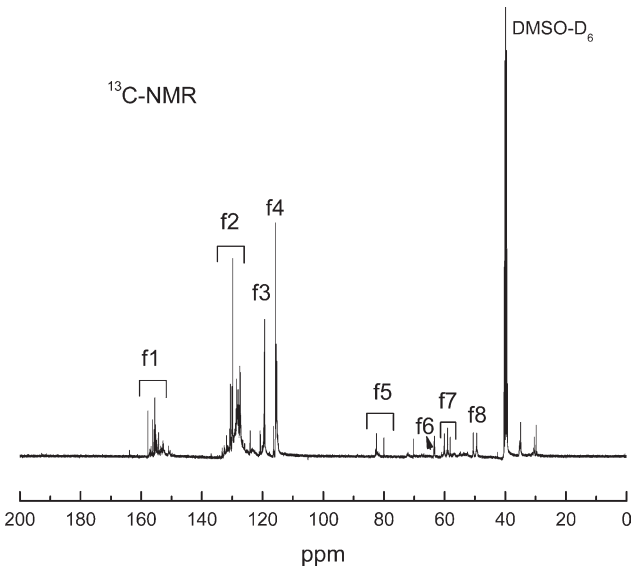

Figure 3 ^{13}C-NMR spectrum of the solid resole (before curing).

linkages of the resole molecules. Figures 2 and 3 present the ^{1}H-NMR and ^{13}C-NMR spectra of the solid resole, respectively, and characteristic chemical shifts and their attributions are listed in Table I. As shown in Figure 2, the chemical shifts at 6.8, 5.19, 4.83, 4.46, and 3.8 ppm were assigned to the resonances of the hydrogen protons of phenyl: f_a, f_b (—CH_2—O—CH_2—OH), f_c (—CH_2—OH), f_d (—CH_2—O—CH_2), and f_e (—CH_2—), respectively.[26] As shown in Figure 3, the NMR resonance signal of f_1 (150–160 ppm) was attributed to the aromatic carbon neighboring the OH groups, and f_2 (122–132 ppm) represented the other aromatic ring carbons.[18] The chemical shifts of the residual characteristic carbons, as marked with an asterisk, are summarized in Table I. From the previous NMR analysis, we concluded that the solid resole contained not only methylol functionalities but also ether functionalities; this was in line with the conclusion from the IR analysis.

GPC

To get information on its molecular weight and distribution [polydispersity index (PDI)], GPC analysis was carried out on the solid resole. Figure 4 plots the GPC curve of the solid resole in tetrahydrofuran, from which several fractions of different molar weights could be identified clearly, as suggested by separate UV signal peaks at different retention times. The molecular weight and its PDI of every fraction are listed in Table II. It is clear that the majority of the fraction (86.8%) had a relatively high molecular weight and a broader distribution. In contrast, fractions 2, 3, and 4 were probably attributable to the monomer, dimer, and trimer, which comprised one, two, and three phenol nuclei, respectively, with their total amount not exceeding 13.2%. These results likely suggest that the studied resole had a great enough molecular weight to account for its amorphous solid state at room temperature compared to conventional liquid resoles with very low molecular

TABLE I
Chemical Shifts of the Characteristic Carbons of the Solid Resole

	Chemical shift (ppm)	Assignment
f_1	150–160	Aromatic carbon neighboring the OH groups
f_2	122–132	Remaining aromatic ring carbons
f_3	120	Free *para*-carbons
f_4	115	Free *ortho*-carbons
f_5	75–85	Oxymethylene (——CH_2——O——$\overset{\star}{C}H_2$——)
f_6	63	Dibenzyl ether bridge carbons (Ar—$CH_2O\overset{\star}{C}H_2$—Ar)
f_7	56–61	Ethers (—$\overset{\star}{C}H_2$—O—CH_2OH)
f_8	50	Methylols (Ar$\overset{\star}{C}H_2OH$)

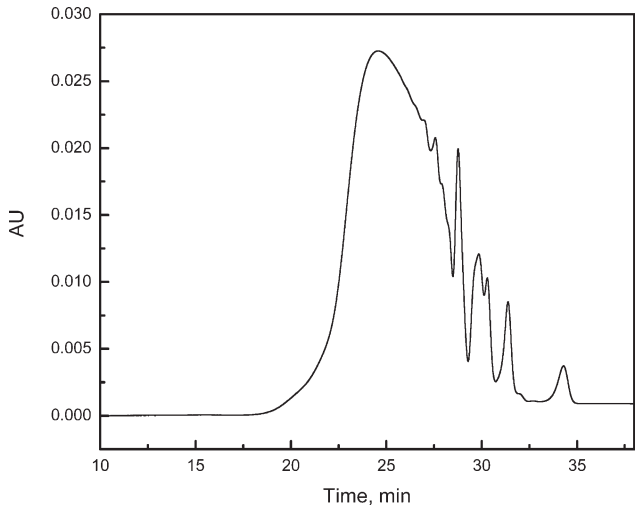

Figure 4 GPC curve of the solid resole with tetrahydrofuran as the eluent (before curing).

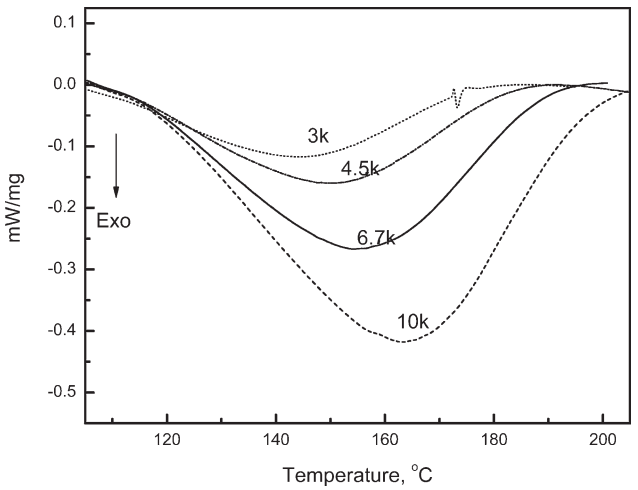

Figure 5 Dynamic DSC curves for the solid resole phenolic resin at 3, 4.5, 6.7, and 10°C/min.

weights (a few hundred).[15] Thus, we concluded that the molecular weight was a decisive factor in determining the resulting resoles in solid or liquid form at room temperature and that it would also be desirable for manufacturers to reduce the contents of low molecular fractions in solid resoles.

Curing reaction

DSC

DSC thermograms of the solid resole at different βs of 3, 4.5, 6.7, and 10°C/min are shown in Figure 5. The calculated reaction onset, peak, and end temperatures (T_{onset}, T_p, and T_{end}, respectively) and the reaction enthalpy (ΔH) are listed in Table III. There was only a single exothermic peak without any shoulder for each nonisothermal run at different βs. Increasing β resulted in the exothermic peak shifting toward a higher temperature range with enlarged peak areas, but reaction exotherms had little dependence on β applied, with no derivation exceeding 15% of their averaged value of 114.6 J/g. These findings implied a reduced reaction time with increasing β but no discernable change in the mechanism during the self-polycondensation reaction of the solid resole. To be more specific, as β increased, the reaction time at a given temperature decreased; this led to an increasing partial percentage of the reaction taking place at a higher temperature with a broader range, but the reaction mechanism was govern by the chemical nature of the resole.

Optimization of the processing temperatures

Further analysis of the DSC thermal traces of the solid resole (Fig. 5) suggested that the exothermic temperatures (T_{onset}, T_p, and T_{end}) increased with β. T_{onset}, T_p, and T_{end} as a function of β are drawn in Figure 6, wherein a good linear correlation can be observed. The limiting values of T_{onset}, T_p, and T_{end} (T^0_{onset}, T^0_p, and T^0_{end}, respectively) were obtained by the extrapolation of β to zero, and their values are summarized in Table IV. According to the literature,[27] T^0_{onset} can be assumed to be equal approximately to the gel temperature, T^0_p is the optimal curing temperature, and T^0_{end} is the end temperature. Thus, the appropriate curing and molding temperature ranges for the solid resole could be determined in reference to the values of T^0_{onset}, T^0_p, and T^0_{end}. In practice, these temperatures can serve as a very useful indicator for determining the optimal processing parameters for resulting phenolic molding materials according to different customers.

TABLE II
Retention Times, Fractions, Number-Average Molecular Weights, Weight-Average Molecular Weights, and PDIs of the Solid Resole

	Retention time (time)	Fraction (%)	Number-average molecular weight	Weight-average molecular weight	PDI
1	24.524	86.84	1038	1727	1.66
2	27.732	6.70	274	279	1.02
3	28.769	5.20	171	173	1.01
4	29.635	1.25	89	90	1.01

TABLE III
Dynamic DSC Data for the Solid Resole Phenolic Resin at Different βs

β (°C/min)	T_{onset} (°C)	T_p (°C)	T_{end} (°C)	ΔH (J/g)
3	102.9	139.5	172.9	105.8
4.5	106.4	147.5	173.0	103.3
6.7	109.8	152.3	187.6	119.8
10	114.3	162.4	195.7	129.3

Activation energy

As indicated in Figure 5, T_p was related closely to β and exhibited a positive correlation. This dependency could be described quantitatively with the relation first proposed by Kissinger,[28,29] as can be written in the following equation:

$$\frac{E\beta}{RT_p^2} = A\exp\left(\frac{-E}{RT_p}\right) \quad (1)$$

where A is the pre-exponential factor (min^{-1}), β is the heating rate (°C/min), T_p is the peak temperature of the dynamic DSC runs (K), R is the gas constant (8.314 J/mol k), and E is the activation energy (J/mol). Equation (1) takes the assumption that the maximum curing reaction rate is achieved at exothermic T_p's.

The frequently cited Kissinger equation is derived from the logarithm of Eq. (1), by which the overall activation energies for a nonisothermal curing reaction can be calculated:

$$-\ln\left(\frac{\beta}{T_p^2}\right) = -\ln\left(\frac{AR}{E}\right) + \frac{E}{RT_p} \quad (2)$$

In this study, the Kissinger equation was used to estimate the global activation energy of the nonisothermal curing reaction of the solid resole. A straight line resulted (Fig. 7) when we plotted $-\ln(\beta/T_p^2)$ versus $1/T_p$. Then, the calculated values of the slope yielded E/R, and the y-intercept line gave rise to the pre-exponential factor. As a result, the values of the global activation energy and the pre-exponential factor could be obtained from Figure 7 by application of the Kissinger method. Their values were 73.23 kJ/mol and 2.92×10^8/min, respectively. The activation value was comparable to that of liquid resoles,[24] which implied that both liquid and solid resoles follow a similar curing mechanism.

TABLE IV
T^0_{onset}, T^0_p, and T^0_{end} Values of the Solid Resole

	Value (°C)	R^2
T^0_{onset}	98.7	0.9936
T^0_p	131.6	0.9894
T^0_{end}	160.6	0.9657

Reaction order (n)

We determined the activation energy of the curing reaction of the resole under nonisothermal conditions. It was necessary to obtain the value of n to achieve an explicit rate equation. Herein, we applied the Crane equation[30,31] to estimate the value of n; it can be expressed by the following equation:

$$\frac{d(\ln\beta)}{d(1/T_p)} = -\left[\frac{E_a}{nR} + 2T_p\right] \quad (3)$$

Where E_a is the activation energy (J/mol). For $\frac{E_a}{nR} \gg 2T_p$, the Crane equation can be reduced to the following equation:

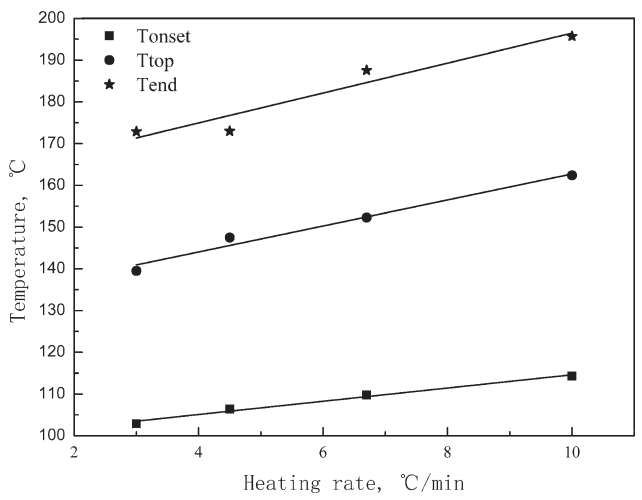

Figure 6 Relationship between the curing temperatures and βs of the solid resole phenolic resin.

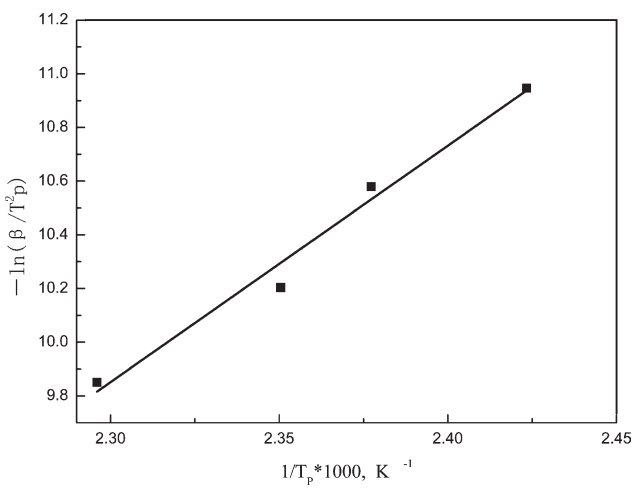

Figure 7 Plot of $-\ln(\beta/T_p^2)$ versus T_p^{-1} for the solid resole.

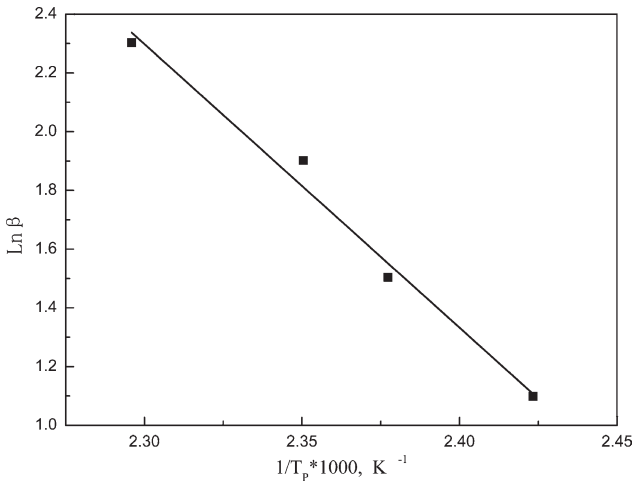

Figure 8 Plot of ln β versus T_p^{-1} for the solid resole.

$$\frac{d(\text{In }\beta)}{d(1/T_p)} = -\frac{E_a}{nR} \tag{4}$$

According to Eq. (4), a plot of ln β against $1/T_p$ yields a straight line, as shown in Figure 8. As a result, if the value of E_a is known, the n value can be reasonably evaluated from the slope of the fit line.

Curing rate equation

To describe the curing reaction of the solid resole quantitatively, the nth-order reaction model[32] is applied in the following kinetics modeling. For the nth-order model, the explicit form of the rate equation for nth-order reactions is shown by Eq. (5).

$$\frac{d\alpha}{dt} = A\exp\left(-\frac{E_a}{RT}\right)(1-\alpha)^n \tag{5}$$

Where a is the degree of curing, t is the reaction time (min), and T is the reaction temperature (K). Substitution into Eq. (5) of the obtained reaction kinetics parameter yields

$$\frac{d\alpha}{dt} = 2.92\times10^8\exp\left(-\frac{7.323\times10^4}{RT}\right)(1-\alpha)^{0.92} \tag{6}$$

Modeling of the curing reaction

For $0.9 < n < 1.1$, the reaction of the solid resole could be approximately considered to be a first-order reaction. Thus, the curing reaction characteristics of the solid resole at constant temperature could be predicted with the simplified rate equation [Eq. (6)] as $n = 1$. When a given degree of curing is reached, the curing reaction time and temperature can be described by the relationship derived from the integral form of Eq. (6)[27]:

$$t = \frac{-\ln(1-\alpha)}{A\exp(-E_a/RT)} \tag{7}$$

With different degrees of curing substituted into Eq. (7), the dependence of the curing time on the temperature at different conversions was calculated, as shown in Figure 9. Evidently, there existed two main pathways to reach the same degree of curing: (1) increasing the curing reaction temperature to shorten the reaction time and (2) prolonging the reaction time to lower the reaction temperature.

Similarly, the relationship between the conversion and the reaction time at different temperatures could be achieved by a slight transformation of Eq. (7), as expressed as follows:

$$\alpha = 1 - \exp[-At\exp(-E_a/RT)] \tag{8}$$

The predicted degree of curing as a function of time for different temperatures is described in Figure 10, from which it is obvious that the higher the curing temperature was, the shorter the curing time was for a given degree of curing.

For the nonisothermal reaction of the solid resole, the degree of curing was governed by two main factors: the reaction time and the reaction temperature, which was closely related to β. The integration of Eq. (8) from the initial temperature (T_0) to a specific degree of curing led to the relation between the conversion and curing temperature at different βs, as expressed by

$$\alpha = 1 - \exp\left[-A\frac{T-T_0}{\beta}\exp(-E_a/RT)\right] \tag{9}$$

The degree of curing as a function of temperature for different βs are plotted in Figure 11, according to Eq. (9). It was demonstrated that the solid resole

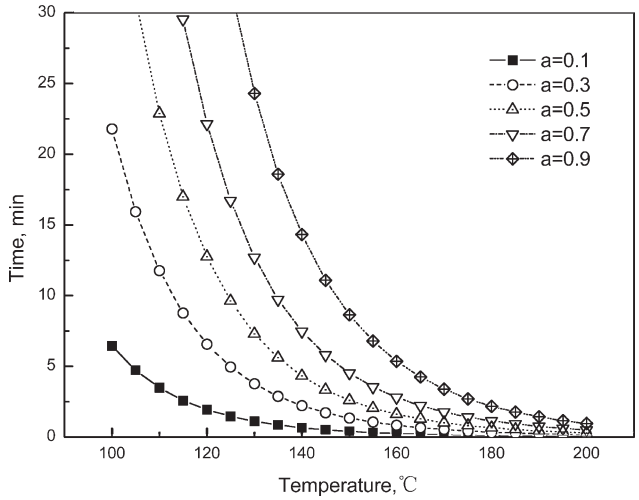

Figure 9 Dependence of the curing time on the temperature for different conversions (a's) for the solid resole phenolic resin.

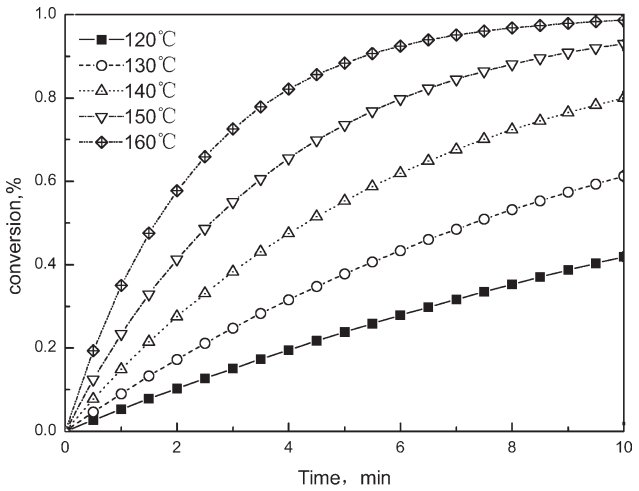

Figure 10 Curves of the conversion versus time at different temperatures for the solid resole phenolic resin.

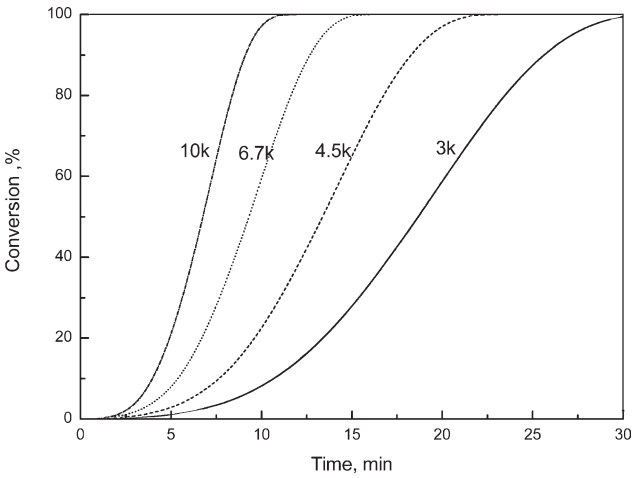

Figure 12 Relationship between the degree of curing and the temperature for the solid resole phenolic resin.

reached an elevated temperature at a higher βs than at lower βs to achieve the same degree of curing. The integration of Eq. (9) from T_0 for a degree of conversion led to the relationship of conversion and curing time at different βs, as written by

$$\alpha = 1 - \exp\{-At\exp[-E_a/R(T_0 + \beta t)]\} \quad (10)$$

The curves of the degree of curing versus time at different βs are shown in Figure 12, according to Eq. (10). It can be drawn from the reaction time that the nonisothermal curing reaction spent a longer time to accomplish the same degree of curing when β was low and vice versa.

When Eq. (5) is combined with Eq. (10), the relationship between the curing rate and the curing reaction time at different βs can be reached:

$$\frac{d\alpha}{dt} = A\exp\left(-\frac{E_a}{R(T_0 + \beta t)}\right)\exp\{-At\exp[-E_a/R \times (T_0 + \beta t)]\} \quad (11)$$

The obtained rate equation [Eq. (11)] could be used to model the curing reaction rate as a function of time at different βs. A straightforward comparison of the curing rate of the solid resole with the simulated result was made, as shown in Figure 13. Clearly, the faster β was, the lower was the curing time needed to achieve the maximum reaction rate. In general, an acceptable match of the curing reaction rates could be achieved with a slight deviation observed when β was slow.

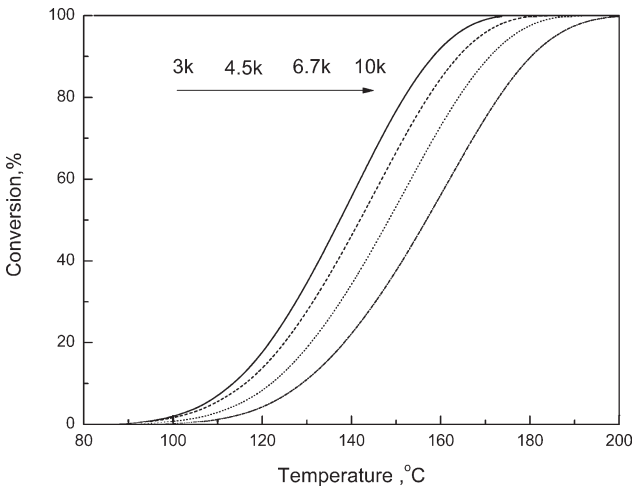

Figure 11 Relationship between the degree of curing and the temperature for the solid resole phenolic resin.

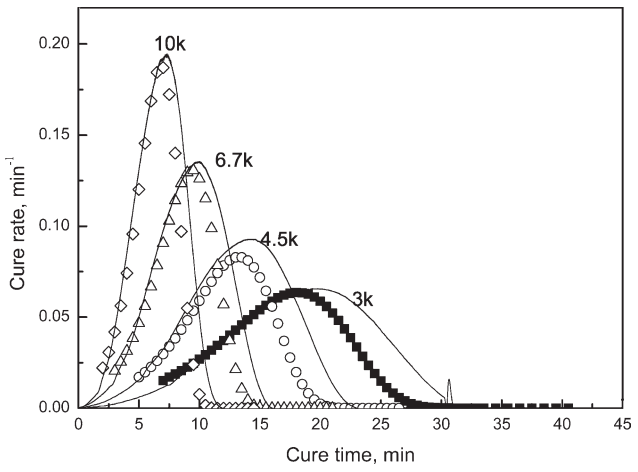

Figure 13 Relationship between the curing rate and the curing time for the solid resole phenolic resin. The dots represent the experimental data, and the lines show prediction.

CONCLUSIONS

The commercial solid resole phenolic resin was characterized systematically with FTIR spectroscopy, NMR, and GPC. The results indicated that the resole had many reactive CH_2—OH and CH_2—O—CH_2 functionalities, which could undergo the curing reaction to produce —CH_2— bridges in the cured solid resole network, and the uncured resole had a great enough molecular weight to maintain their solid state at room temperature. The curing reaction of the resole was investigated with dynamic DSC at different βs. It was found that the reaction exotherms had little dependence on βs, but the reaction rate showed a strong correlation with β. Optimal processing temperatures were obtained from dynamic DSC curves by extrapolating β to zero. The global activation of the nonisothermal curing reaction was determined to be 72.23 kJ/mol with the Kissinger equation, and n was calculated to be 0.92 from the Crane equation. In addition, a first-order reaction model was used to predict the advancement of the curing reaction with an acceptable fit of the reaction rate achieved. In conclusion, in this study, we obtained a fundamental knowledge of the commercial solid resole at a molecular level and its curing reaction from a kinetic perspective. Ongoing work on the solid resole will center on the thermal stability and properties of composite materials based on the solid resole.

References

1. Parameswaran, P. S.; Bhuvaneswary, M. G.; Eby Thomas, T. J Appl Polym Sci 2009, 113, 802.
2. Chiu, H. T.; Chiu, S. H.; Jeng, R. E.; Chung, J. S. Polym Degrad Stab 2000, 70, 505.
3. Reghunadhan Nair, C. P.; Bindu, R. L.; Ninan, K. N. Polym Degrad Stab 2001, 73, 251.
4. Achary, P. S.; Ramaswamy, R. J Appl Polym Sci 1998, 69, 1187.
5. Laza, J. M.; Alonso, J.; Vilas, J. L.; Rodríguez, M.; León, L. M.; Gondra, K.; Ballestero, J. J Appl Polym Sci 2008, 108, 387.
6. Megiatto, J. D., Jr.; Silva, C. G.; Ramires, E. C.; Frollini, E. Polym Test 2009, 28, 793.
7. Mark, J. E. Oxford University Press, Inc.: New York, 1999, 3rd Edition.
8. Shafizadeh, J. E.; Guionnet, S.; Tillman, M. S.; Seferis, J. C. J Appl Polym Sci 1999, 73, 505.
9. Stark, W.; Goering, H.; Michel, U.; Bayerl, H. Polym Test 2009, 28, 561.
10. Gardziella, A.; Pilato, L. A.; Knop, A. Springer: New York, 2000, 2nd Edition.
11. Knop, A.; Pilato, L. A. Springer-Verlag: Berlin, 1985.
12. Sojka, S. A.; Wolfe, R. A.; Guenther, G. D. Macromolecules 1981, 14, 1539.
13. Hatfield, G. R.; Maciel, G. E. Macromolecules 1987, 20, 608.
14. Korošec, R.; Mežnar, L.; Bukovec, P. J Therm Anal Calorim 2009, 95, 235.
15. Gupta, M. K.; Hindersinn, R. R. Polym Eng Sci 1987, 27, 976.
16. Regina-Mazzuca, A. M.; Ark, W. F.; Jones, T. R. Ind Eng Chem Proc Des Dev 1982, 21, 139.
17. Riccardi, C. C.; Aierbe, G. A.; Echeverría, J. M.; Mondragon, I. Polymer 2002, 43, 1631.
18. Solomon, S.; Alfred, R. J Appl Polym Sci 1990, 41, 205.
19. Kaledkowski, B.; Hetper, J. Polymer 2000, 41, 1679.
20. Astarloa-Aierbe, G.; Echeverría, J. M.; Vázquez, A. A.; Mondragon, I. Polymer 2000, 41, 3311.
21. Astarloa-Aierbe, G.; Echeverría, J. M.; Mondragon, I. Polymer 1999, 40, 5873.
22. Focke, W. W.; Smit, M. S.; Tolmay, A. T.; Walt, L. S. V. D.; Wyk, W. L. V. Polym Eng Sci 1991, 31, 1665.
23. Pralay, K. P.; Anil, K.; Santosh, K. G. Polym Int 1980, 12, 121.
24. Gabilondo, N.; López, M.; Ramos, J.; Echeverría, J.; Mondragon, I. J Therm Anal Calorim 2007, 90, 229.
25. Carotenuto, G.; Nicolais, L. J Appl Polym Sci 1999, 74, 2703.
26. Grenier-Loustalot, M.-F.; Larroque, S.; Grenier, P.; Leca, J.-P.; Bedel, D. Polymer 1994, 35, 3046.
27. Xiuni, Z.; Yuexin, D. Acta Mater Compos Sinica 2007, 24, 100.
28. Kissinger, H. E. J Res Natl Bur Stand A 1956, 57, 217.
29. Kissinger, H. E. Anal Chem 1957, 29, 1702.
30. Crane, L. W.; Dynes, P. J.; Kaelble, D. H. J Polym Sci Polym Lett Ed 1973, 11, 533.
31. Liu, W.; Qiu, Q.; Wang, J.; Huo, Z.; Sun, H. Polymer 2008, 49, 4399.
32. Park, B.-D.; Riedl, B.; Hsu, E. W.; Shields, J. Polymer 1999, 40, 1689.